Sādhanā (2020)45:158
https://doi.org/10.1007/s12046-020-01393-3

Investigation of electromagnetic torque production in induction motor during charging operation

SOHIT SHARMA*, MOHAN V AWARE and APEKSHIT BHOWATE

Department of Electrical Engineering, Visvesvaraya National Institute of Technology, Nagpur, India
e-mail: sohitee@students.vnit.ac.in; mvaware@eee.vnit.ac.in; apekshit.bhowate@students.vnit.ac.in

MS received 10 July 2019; revised 2 May 2020; accepted 15 May 2020

Abstract. Integrated battery chargers (IBCs) provide the flexibility of reusing the electric drive-train components of the electric vehicle (EV) for the charging operation. The purpose of the paper is to reuse its traction inverter and motor windings as rectifier and grid interfacing filter, respectively for charging and keeping rotor standstill without using any external brake. Various winding configurations are developed by splitting the three-phase induction motor (IM) winding into two parts at zero electrical degree to keep the rotor standstill. The different stator winding connections are proposed for IM which restricts the formation of rotating magnetic field (RMF). Cases are categorized into two parts, in the first part, RMF is cancelled to zero and in the other part, RMF is converted into pulsating magnetic field (PMF). Mathematical investigation for torque production in both cases is provided to prove that the proposed winding connections are incapable of developing electromagnetic torque in machine. Mathematical findings are validated by experimentation on split three-phase IM (STP-IM). This analysis is useful in identifying the nature of torque developed in motor during charging operation of EV.

Keywords. Integrated battery charger; filter; winding impedance; pulsating magnetic field; electromagnetic torque.

1. Introduction

Battery chargers play a significant role for electric vehicles (EVs). Various battery charger topologies are discussed in [1, 2]. Primarily they are classified as off-board chargers (figures 1(a)) and on-board chargers (figure 1(b)). During conductive charging, on-board driving motor of the EV is stationary and inverter is idle. Hence, the same hardware is used as the charger and is known as integrated battery charger (IBC) as shown in figures 1 ((c) and (d)) where stator windings of machine are used as filter and inverter is used as rectifier. As three-phase supply is being connected to three-phase IM, the rotor of the machine starts rotating. Hence, separate clutch is required to decouple the rotating rotor and wheels of EV as shown in figure 1(c). This method is inefficient as power used for charging the battery is utilized in rotation of IM. The locking of rotor by an external force is also inefficient as it draws high magnetizing current from the grid [3]. The traction motor of EV could be integrated into the charging process in three ways. In first, traction motor (interior permanent magnet motor) is operated as rotating transformer to provide the galvanic isolation between charger and grid [4, 5]. In a second way, stator windings are used as coupled DC inductor where machine carries the current in stator windings such that rotor becomes standstill [6]. Such types of chargers are developed with permanent magnet synchronous motor (PMSM) [7, 8] for single-phase supply. A three-phase supply based charger is discussed in [9] with PMSM.

In third, stator windings are used as a filter between grid and converter. With single-phase supply, electromagnetic torque cancellation process for the machine is similar to the second category [10, 11]. For three-phase supply based chargers, rotor rotation is prevented by reconfiguring the stator windings, ensuring rotor stand-stillness during the charging process as shown in figure 1(d) and the clutch is inessential. The third category of IBC eliminates the need of bulky grid inductive filters. The objective for developing the on-board IBC is to save cost, volume, space and weight in the EV [12, 13]. The first IBC based on SCR was developed for NASA project in 1985 with the major objective of reducing the 50% volume and 30% weight of the first generation inverter power stage [14]. In 2010, on-board charger for EVs based on split-phase motor was introduced by Valeo Power-Train Systems and patented in [15–18]. This charger is based on the three-phase open end topology, where from both side of stator windings, inverters are connected. In such type of chargers, circulating current may flow [19, 20] which causes unwanted losses in the machine windings. The chameleon charger which is commercially used in Renault ZOE uses stator windings as DC coupled inductors [21] and its working is based on patents

*For correspondence
Published online: 18 June 2020

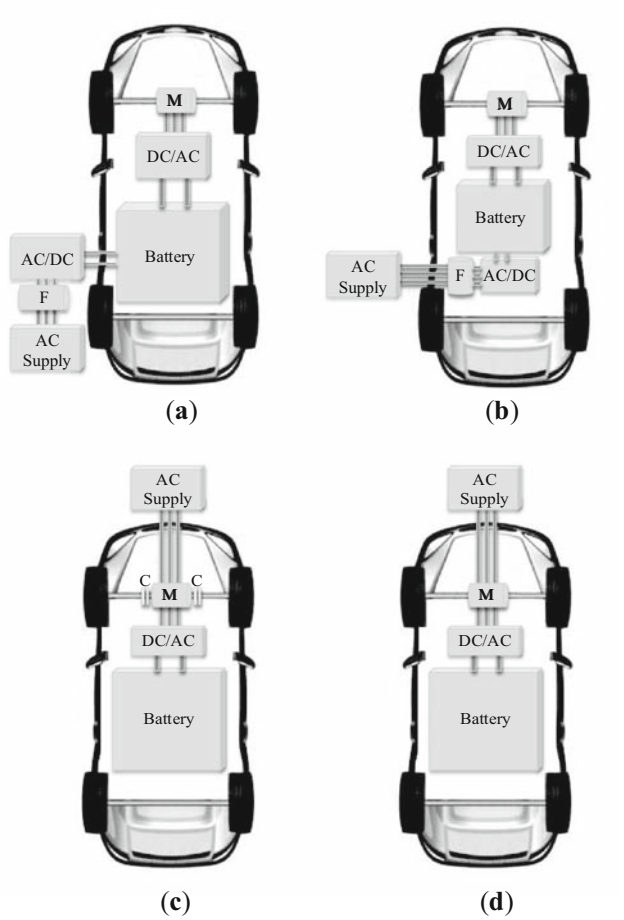

Figure 1. (a) Off-board charger, (b) On-board charger, (c) On-board IBC, (d) On-board IBC without C (M-Motor, F-Filter, C-Clutch).

[22, 23]. For the charging mode, this configuration requires additional components (rectifier).

According to [24], nowadays IMs are the second choice for EVs. However, the advantage of using IM as an integrated motor drive over PMSM is that its winding inductance [25] and developed electromagnetic torque [26] are independent of rotor position. The limited IBC solutions using three-phase IM with three-phase inverter are presented and stated in [10, 27].

The winding connections of split three-phase IM (STP-IM) are proposed for integrating the motoring mode and filtering mode in a single machine by exploiting the conventional machine design [28]. When windings of IM are used as filter between the grid and converter, average electromagnetic torque developed in rotor should be zero. Various possible winding configurations are developed to keep the rotor standstill without using mechanical force during charging mode. In recent developed topologies [19, 28], motor windings are connected in parallel through reconfigurable switches to avoid torque generation in rotor for charging operation. The developed connections are different from the previously discussed connections in literature because proposed windings are connected in series. Hence, no circulating current will flow in the machine and will provide higher inductance for filtering during charging. These connections are verified by mathematical expressions to ensure that average electromagnetic torque developed by motor is zero. The impact of inductance matrices on derived torque equation is elaborated and these equations provide the rotor status (stationary/rotating). The PMF in motor produces the pulsating torque which is incapable to rotate the rotor however it changes the equivalent winding parameters used for filtering. The ratio of winding inductance and resistance (X/R ratio) is observed for the connections (for stationary rotor) to find the most suitable configuration for charging operation. Its impact on current flowing through the filter is also analyzed.

2. Split three-phase induction motor

The STP-IM has two three-phase windings with zero degree displacement. All developed cases are shown in figure 2. In case-I, both windings are connected in series such that current leaves from dot of winding, means windings are connected in same sense of orientation. When balanced three-phase current flows through these windings as shown in figure 3, it develops flux in motor presented in figure 4(a) at six instants. The flux Φ is generated when winding carries peak current. The direction of flux is along with the phase when the current is positive. The direction of flux is opposite when the current is negative. These phasors depict that developed field rotates from leading phase to lagging phase. When this RMF interacts with rotor windings, produces torque in machine.

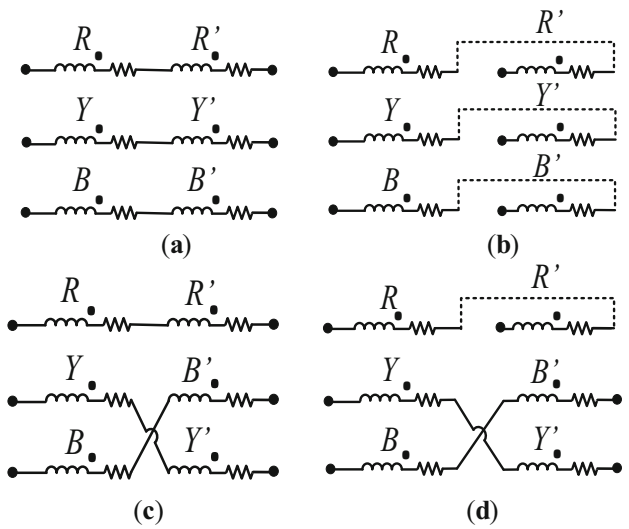

Figure 2. Windings configurations (a) Case-I, (b) Case-II, (c) Case-III, (d) Case-IV.

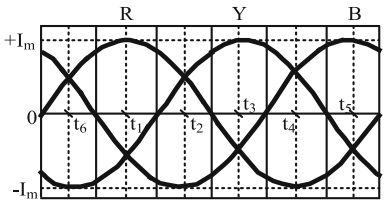

Figure 3. Three-phase current flowing in machine windings.

In case-II (figure 2(b)), current leaves through the dot in one winding and it enters through the dot in second winding, means windings are connected in *opposite sense of orientation*. When second three-phase winding is connected in *opposite sense of orientation* then field created by one winding is cancelled by other as shown in figure 4(b). Therefore, there is no magnetic linkage between stator and rotor of the machine. Hence rotor is stationary. In case-III, both windings are connected in series having *opposite phase-sequence of supply*. The first phase of second winding is connected to the first phase of the first winding but second and third winding connections are interchanged as shown in figure 2(c).

Since, the R-phase connection is common in both windings, flux formed in this case is along R-phase axis for all six instants as shown in figure 4(c). This PMF is incapable to generate the electromagnetic torque for rotating the rotor. The magnitude of PMF is further reduced by connecting the second R-phase winding in *opposite sense of orientation* as shown in figure 2(d). This case is named as case-IV. The flux production is shown in figure 4(d).

3. Electromagnetic torque equation for winding configurations

In the developed equations, following assumptions are considered.

1. The air gap in IM is uniform.
2. The windings are sinusoidally distributed along the air gap.
3. Both the three-phase windings are identical.
4. Losses (eddy current, friction, and windage) and magnetic saturation are neglected.

Torque expression is formulated by assuming that rotor is having similar nature of field as of stator due to transformer action. For incorporating the effect of PMF in the mathematical expression on the rotor side, its connections are also represented same as that of stator. However, in actual IM there is only one rotor. Voltage equations for stator, and rotor of IM can be written as (1) and (2) respectively (where $p = {}^{d}/_{dt}$).

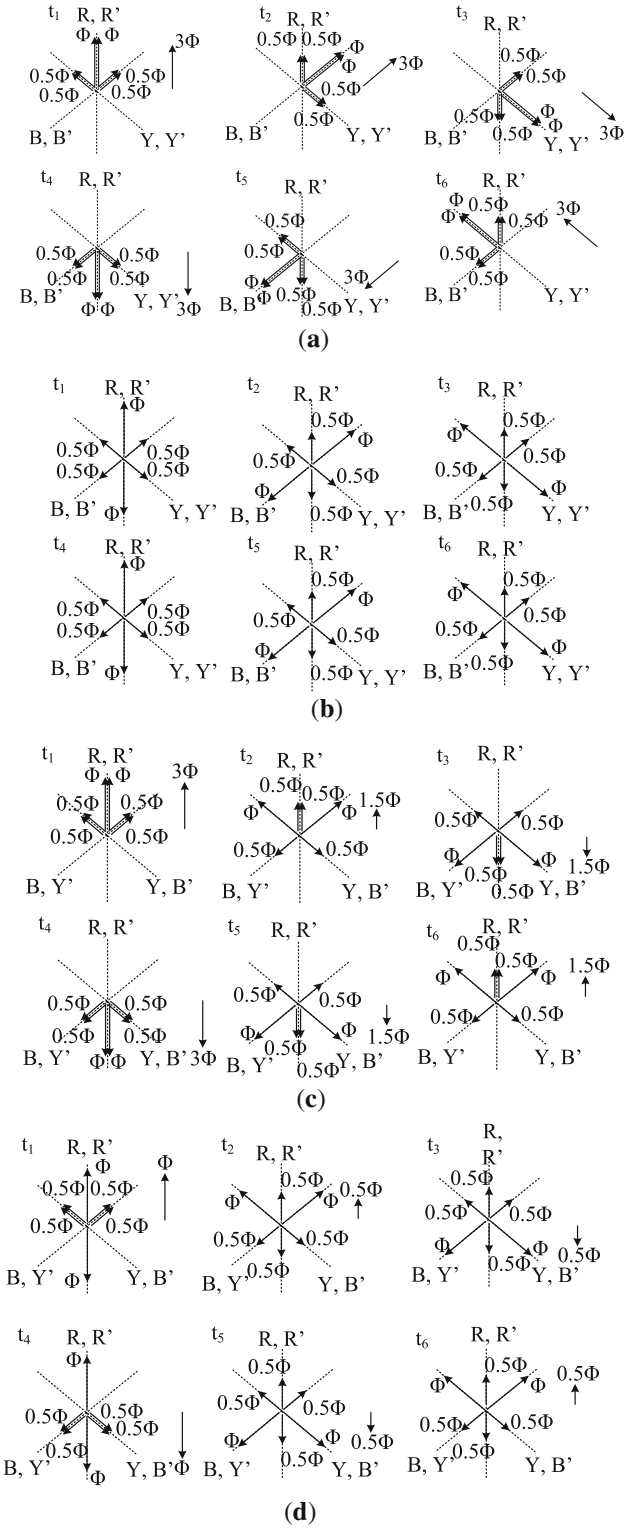

Figure 4. Flux formation (a) Case-I, (b) Case-II, (c) Case-III, (d) Case-IV.

$$[v_s] = [R_s][i_s] + p([L_{ss}][i_s] + [L_{sr}][i_r]) \quad (1)$$

$$[v_r] = [R_r][i_r] + p([L_{rr}][i_r] + [L_{rs}][i_s]) \quad (2)$$

These equations are in abc-form. By using stationary dq-transformation (1), and (2) are converted in two-phase form (subscript '*dq*' represents variables in dq-frame and superscript '*r*' shows the rotor axes).

$$\left[v_{s\_dq}\right] = \left[R_{s\_dq}\right]\left[i_{s\_dq}\right] + p\left(\left[L_{ss\_dq}\right]\left[i_{s\_dq}\right] + \left[L_{sr\_dq}\right]\left[i^{r}_{r\_dq}\right]\right) \quad (3)$$

$$\left[v^{r}_{r\_dq}\right] = \left[R_{r\_dq}\right]\left[i^{r}_{r\_dq}\right] + p\left(\left[L_{rr\_dq}\right]\left[i^{r}_{r\_dq}\right] + \left[L_{rs\_dq}\right]\left[i_{s\_dq}\right]\right) \quad (4)$$

In ((3) and (4)), inductances are the time-varying quantities. Therefore, for obtaining the constant inductances, actual rotor axes are replaced by the fictitious axes with transformation matrix (5) where X could be voltage or current.

$$\begin{bmatrix} X^{r}_{dr} \\ X^{r}_{qr} \\ X^{r}_{0r} \end{bmatrix} = \begin{bmatrix} \cos(\theta_r) & \sin(\theta_r) & 0 \\ -\sin(\theta_r) & \cos(\theta_r) & 0 \\ 0 & 0 & 1 \end{bmatrix} \begin{bmatrix} X_{dr} \\ X_{qr} \\ X_{0r} \end{bmatrix} = [T] \begin{bmatrix} X_{dr} \\ X_{qr} \\ X_{0r} \end{bmatrix} \quad (5)$$

$$\left[v_{s\_dq}\right] = \left[R_{s\_dq}\right]\left[i_{s\_dq}\right] + p\left(\left[L_{ss\_dq}\right]\left[i_{s\_dq}\right] + \left[L_{sr\_dq}\right][T]\left[i_{r\_dq}\right]\right) \quad (6)$$

$$\left[v_{r\_dq}\right] = [T]^{-1}\left[R_{r\_dq}\right][T]\left[i_{r\_dq}\right] + [T]^{-1}p\left(\left[L_{rr\_dq}\right][T]\left[i_{r\_dq}\right] + \left[L_{rs\_dq}\right]\left[i_{s\_dq}\right]\right) \quad (7)$$

By using eqs. (6), and (7), torque expression is developed and time-varying inductances are converted into constant terms. This approach is used to calculate the torque expression for all cases. As the winding configuration is modified, accordingly variables used in (1), (2) are also modified. The final torque equation is obtained by using (6) and (7).

3.1 *Case-I: Motoring connection*

Figure 5(a) shows the connections for the case-I. Rotor windings are displaced by θ_r from the stator windings as shown in figure 5(b).

Voltage equations for the stator and rotor circuit are presented in eqs. (8) and (9), respectively, where r_s, r_r, L_{ls}, L_{lr}, and L_m are the stator resistance, rotor resistance, stator leakage inductance, rotor leakage inductance, and mutual inductance respectively. The formulation of (8) and (9) is provided in Appendix A.

$$\begin{bmatrix} v_{ds} \\ v_{qs} \\ v_{0s} \end{bmatrix} = \begin{bmatrix} 2r_s & 0 & 0 \\ 0 & 2r_s & 0 \\ 0 & 0 & 2r_s \end{bmatrix} \begin{bmatrix} i_{ds} \\ i_{qs} \\ i_{0s} \end{bmatrix} + \begin{bmatrix} 2L_{ls}+6L_m & 0 & 0 \\ 0 & 2L_{ls}+6L_m & 0 \\ 0 & 0 & 2L_{ls} \end{bmatrix} \begin{bmatrix} pi_{ds} \\ pi_{qs} \\ pi_{0s} \end{bmatrix} + \begin{bmatrix} 6L_m & 0 & 0 \\ 0 & 6L_m & 0 \\ 0 & 0 & 0 \end{bmatrix} \begin{bmatrix} pi_{dr} \\ pi_{qr} \\ pi_{0r} \end{bmatrix} \quad (8)$$

$$\begin{bmatrix} v_{dr} \\ v_{qr} \\ v_{0r} \end{bmatrix} = \begin{bmatrix} 2r_r & 0 & 0 \\ 0 & 2r_r & 0 \\ 0 & 0 & 2r_r \end{bmatrix} \begin{bmatrix} i_{dr} \\ i_{qr} \\ i_{0r} \end{bmatrix} + \begin{bmatrix} 2L_{lr}+6L_m & 0 & 0 \\ 0 & 2L_{lr}+6L_m & 0 \\ 0 & 0 & 2L_{lr} \end{bmatrix} \begin{bmatrix} pi_{dr} \\ pi_{qr} \\ pi_{0r} \end{bmatrix} + \begin{bmatrix} 0 & (2L_{lr}+6L_m)\omega_r & 0 \\ -(2L_{lr}+6L_m)\omega_r & 0 & 0 \\ 0 & 0 & 0 \end{bmatrix} \begin{bmatrix} i_{dr} \\ i_{qr} \\ i_{0r} \end{bmatrix} + \begin{bmatrix} 6L_m & 0 & 0 \\ 0 & 6L_m & 0 \\ 0 & 0 & 0 \end{bmatrix} \begin{bmatrix} pi_{ds} \\ pi_{qs} \\ pi_{0s} \end{bmatrix} + \begin{bmatrix} 0 & 6L_m\omega_r & 0 \\ -6L_m\omega_r & 0 & 0 \\ 0 & 0 & 0 \end{bmatrix} \begin{bmatrix} i_{ds} \\ i_{qs} \\ i_{0s} \end{bmatrix} \quad (9)$$

The electromagnetic torque can be written from (8) and (9) as,

$$T_e = 3PL_m\left(i_{qs}i_{dr} - i_{ds}i_{qr}\right) \quad (10)$$

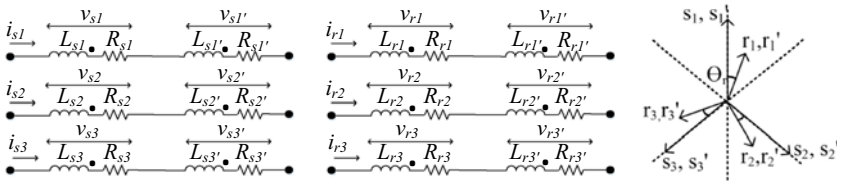

(a) **(b)**

Figure 5. (a) Case-I: Stator and rotor windings and (b) Windings axes of STP-IM.

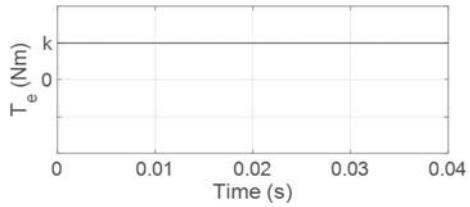

Figure 6. Case-I: Electromagnetic torque.

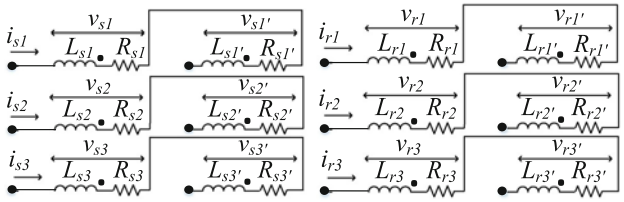

Figure 7. Case-II: Stator and rotor windings.

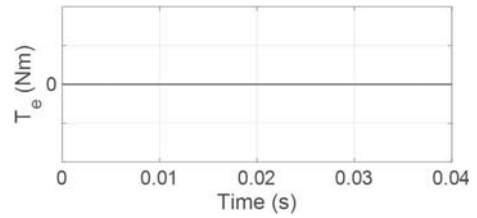

Figure 8. Case-II: Electromagnetic torque.

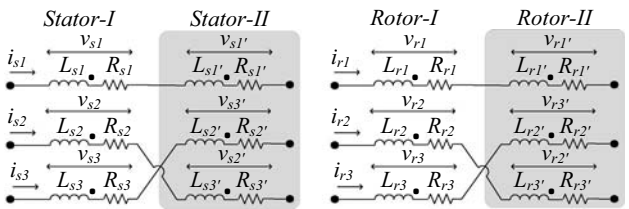

Figure 9. Case-III: Stator and rotor windings.

Assuming in two pole IM, stator carries the balanced three-phase current with peak I_s and rotor carries the current I_r having a phase angle of θ with respect to stator current, then from (10), T_e is calculated as $9L_mI_sI_r \sin\theta$. If the phase angle between stator and rotor current is 90°, then maximum electromagnetic torque is obtained. The torque value is positive constant for the constant stator current as in (11) and shown in figure 6.

$$T_e = k \quad (\text{where}, k = 9L_mI_sI_r) \tag{11}$$

Hence, rotor rotates in case-I. It is observed from (10) that for generating torque, product term of both currents should be in quadrature and one current is from stator, and other is from rotor. But if stator of IM having single-phase supply as given in [10, 11] then $i_{ds} = i_{qs} = 0$. Therefore, electromagnetic torque for single-phase supply is zero and rotor is standstill.

3.2 *Case-II: Opposite sense of orientation*

In case-II, current enters through dot in one winding and it leaves through dot in other as shown in figure 7.

Voltage equation for stator (12) and rotor (13), shows that there is no mutual terms present between stator and rotor (Appendix B).

$$\begin{bmatrix} v_{ds} \\ v_{qs} \\ v_{0s} \end{bmatrix} = \begin{bmatrix} 2r_s & 0 & 0 \\ 0 & 2r_s & 0 \\ 0 & 0 & 2r_s \end{bmatrix} \begin{bmatrix} i_{ds} \\ i_{qs} \\ i_{0s} \end{bmatrix} + \begin{bmatrix} 2L_{ls} & 0 & 0 \\ 0 & 2L_{ls} & 0 \\ 0 & 0 & 2L_{ls} \end{bmatrix} \begin{bmatrix} pi_{ds} \\ pi_{qs} \\ pi_{0s} \end{bmatrix} \tag{12}$$

$$\begin{bmatrix} v_{dr} \\ v_{qr} \\ v_{0r} \end{bmatrix} = \begin{bmatrix} 2r_r & 0 & 0 \\ 0 & 2r_r & 0 \\ 0 & 0 & 2r_r \end{bmatrix} \begin{bmatrix} i_{dr} \\ i_{qr} \\ i_{0r} \end{bmatrix} + \begin{bmatrix} 2L_{lr} & 0 & 0 \\ 0 & 2L_{lr} & 0 \\ 0 & 0 & 2L_{lr} \end{bmatrix} \begin{bmatrix} pi_{dr} \\ pi_{qr} \\ pi_{0r} \end{bmatrix} \tag{13}$$

The electromagnetic torque developed in this case is zero. Therefore,

$$T_e = 0 \tag{14}$$

This condition confirms that the field developed by one winding is cancelled by other winding, leading to zero electromagnetic torque production as presented in figure 8.

3.3 *Case-III: Opposite phase-sequence of supply*

In case-III, as shown in figure 9, half stator windings are supplied by *opposite phase-sequence of supply*. The torque expression for such cases are developed by formulating two torque equations, i.e., one for each phase-sequence supply.

For stator-I and rotor-I windings, voltage equations (15), and (16) are mentioned below (refer to Appendix C):

$$\begin{bmatrix} v_{ds1} \\ v_{qs1} \\ v_{0s1} \end{bmatrix} = \begin{bmatrix} r_s & 0 & 0 \\ 0 & r_s & 0 \\ 0 & 0 & r_s \end{bmatrix} \begin{bmatrix} i_{ds1} \\ i_{qs1} \\ i_{0s1} \end{bmatrix} + \begin{bmatrix} L_{ls} + 3L_m & 0 & 0 \\ 0 & L_{ls} & 0 \\ 0 & 0 & L_{ls} \end{bmatrix} \begin{bmatrix} pi_{ds1} \\ pi_{qs1} \\ pi_{0s1} \end{bmatrix} + \begin{bmatrix} 3L_m cos^2(\theta_r) & 1.5L_m \sin(2\theta_r) & 0 \\ 1.5L_m \sin(2\theta_r) & 3L_m sin^2(\theta_r) & 0 \\ 0 & 0 & 0 \end{bmatrix} \begin{bmatrix} pi_{ds1} \\ pi_{qs1} \\ pi_{0s1} \end{bmatrix} + \begin{bmatrix} -3L_m\omega_r \sin(2\theta_r) & 3L_m\omega_r \cos(2\theta_r) & 0 \\ 3L_m\omega_r \cos(2\theta_r) & 3L_m\omega_r \sin(2\theta_r) & 0 \\ 0 & 0 & 0 \end{bmatrix} \begin{bmatrix} i_{dr1} \\ i_{qr1} \\ i_{0r1} \end{bmatrix} \tag{15}$$

$$\begin{bmatrix} v_{dr1} \\ v_{qr1} \\ v_{0r1} \end{bmatrix} = \begin{bmatrix} r_r & 0 & 0 \\ 0 & r_r & 0 \\ 0 & 0 & r_r \end{bmatrix} \begin{bmatrix} i_{dr1} \\ i_{qr1} \\ i_{0r1} \end{bmatrix} + \begin{bmatrix} L_{lr} + 3L_m cos^2(\theta_r) & 1.5L_m\omega_r \sin(2\theta_r) & 0 \\ 1.5L_m\omega_r \sin(2\theta_r) & L_{lr} + 3L_m sin^2(\theta_r) & 0 \\ 0 & 0 & L_{lr} \end{bmatrix} \begin{bmatrix} pi_{dr1} \\ pi_{qr1} \\ pi_{0r1} \end{bmatrix} + \begin{bmatrix} -1.5L_m\omega_r \sin(2\theta_r) & L_{lr}\omega_r + 3L_m\omega_r cos^2(\theta_r) & 0 \\ -L_{lr}\omega_r - 3L_m\omega_r sin^2(\theta_r) & 1.5L_m\omega_r \sin(2\theta_r) & 0 \\ 0 & 0 & 0 \end{bmatrix} \begin{bmatrix} i_{dr1} \\ i_{qr1} \\ i_{0r1} \end{bmatrix} + \begin{bmatrix} 3L_m & 0 & 0 \\ 0 & 0 & 0 \\ 0 & 0 & 0 \end{bmatrix} \begin{bmatrix} pi_{ds1} \\ pi_{qs1} \\ pi_{0s1} \end{bmatrix} + \begin{bmatrix} 0 & 0 & 0 \\ -3L_m\omega_r & 0 & 0 \\ 0 & 0 & 0 \end{bmatrix} \begin{bmatrix} i_{ds1} \\ i_{qs1} \\ i_{0s1} \end{bmatrix} \tag{16}$$

The first torque expression is formed by considering first half of stator and rotor windings as presented in (17).

$$\begin{aligned} T_{e-I} = (P/2)\big[&-3L_m \sin(2\theta_r) i_{ds1} i_{dr1} + 3L_m \cos(2\theta_r) i_{ds1} i_{qr1} \\ &+3L_m \cos(2\theta_r) i_{qs1} i_{dr1} \\ &+ \ 3L_m \sin(2\theta_r) i_{qs1} i_{qr1} - 1.5L_m \sin(2\theta_r) i_{dr1}^2 \\ &+3L_m \cos(2\theta_r) i_{dr1} i_{qr1} + 1.5L_m \sin(2\theta_r) i_{qr1}^2 \\ &- 3L_m i_{ds1} i_{qr1}\big] \end{aligned} \tag{17}$$

The second expression is developed by taking other half of stator and rotor windings. It is observed that final voltage equations are similar as (15) and (16). Due to opposite phase-sequence, voltage and current in dq-frame are not same as of (stator-I and rotor-I). Therefore, for stator-II and rotor-II, these terms are written with subscript '2'. For stator-II and rotor-II, torque equation shown in (18).

$$\begin{aligned} T_{e-II} = (P/2)\big[&-3L_m \sin(2\theta_r) i_{ds2} i_{dr2} + 3L_m \cos(2\theta_r) i_{ds2} i_{qr2} \\ &+3L_m \cos(2\theta_r) i_{qs2} i_{dr2} \\ &+ \ 3L_m \sin(2\theta_r) i_{qs2} i_{qr2} - 1.5L_m \sin(2\theta_r) i_{dr2}^2 \\ &+3L_m \cos(2\theta_r) i_{dr2} i_{qr2} + 1.5L_m \sin(2\theta_r) i_{qr2}^2 \\ &- 3L_m i_{ds2} i_{qr2}\big] \end{aligned} \tag{18}$$

$T_{e\text{-}I}$ gives torque for first half stator windings and $T_{e\text{-}II}$ provides the torque for other half stator windings. Stator-I and stator-II windings are having different *phase-sequence of supply*, therefore (19) shows the relationship between the dq variables for both the windings.

$$\begin{aligned} &i_{ds} = i_{ds1} = i_{ds2}, \quad i_{dr} = i_{dr1} = i_{dr2} \\ &i_{qs} = i_{qs1} = -i_{qs2}, \quad i_{qr} = i_{qr1} = -i_{qr2} \\ &i_{0s} = i_{0s1} = i_{0s2}, \quad i_{0r} = i_{0r1} = i_{0r2} \end{aligned} \tag{19}$$

By adding both torques, final resultant is obtained and given by (20).

$$\begin{aligned} T_e &= T_{e-I} + T_{e-II} \\ T_e &= 1.5PL_m \sin(2\theta_r)\left[2\left(i_{qs} i_{qr} - i_{ds} i_{dr}\right) + \left(i_{qr}^2 - i_{dr}^2\right)\right] \end{aligned} \tag{20}$$

From this expression, it is observed that there is no multiplication of quadrature current. After assuming balanced sinusoidal current with phase difference of 90° for stator and rotor of two pole IM, then (20) is converted into (21).

$$T_e = k_1 \sin(2\omega t) - k_2 \cos(2\omega t) \tag{21}$$

where $k_1 = 9L_m I_s I_r \sin(2\theta_r)$,$k_2 = 4.5L_m I_r^2 \sin(2\theta_r)$

Here θ_r is constant, therefore double frequency ($2\omega t$) component is present in T_e. The electromagnetic torque developed in case-III will oscillate around zero axis with double frequency oscillations as shown in figure 10.

It is justified from (21), that nature of torque in case-III is of pulsating nature which is incapable to rotate the rotor. If θ_r is made equal to ωt by using external force on the rotor then average value of this torque is non-zero which rotates the rotor. The magnitude of the pulsating torque could be reduced by reducing the magnitude of PMF. This can be obtained by connecting the R-phase windings in *opposite sense of orientation*. This case is discussed in next section.

3.4 *Case-IV: (Combination of case-II and case-III)*

The torque equation for this case is also obtained by using the same approach as of case-III and winding connection is shown in figure 11.

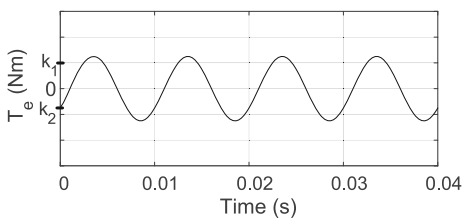

Figure 10. Case-III: Electromagnetic torque.

$T_{e\text{-}I}$ is calculated for the stator-I and rotor-I. The voltage equations (22) and (23) are shown below (for detail refer Appendix-D).

$$\begin{bmatrix} v_{ds1} \\ v_{qs1} \\ v_{0s1} \end{bmatrix} = \begin{bmatrix} r_s & 0 & 0 \\ 0 & r_s & 0 \\ 0 & 0 & r_s \end{bmatrix} \begin{bmatrix} i_{ds1} \\ i_{qs1} \\ i_{0s1} \end{bmatrix} + \begin{bmatrix} L_{ls}+L_m & 0 & -\sqrt{2}L_m \\ 0 & L_{ls} & 0 \\ 0 & 0 & L_{ls} \end{bmatrix} \begin{bmatrix} pi_{ds1} \\ pi_{qs1} \\ pi_{0s1} \end{bmatrix} + \begin{bmatrix} L_m cos^2(\theta_r) & 0.5L_m \sin(2\theta_r) & -\sqrt{2}L_m \cos(\theta_r) \\ 0.5L_m \sin(2\theta_r) & L_m sin^2(\theta_r) & -\sqrt{2}L_m \sin(\theta_r) \\ 0 & 0 & 0 \end{bmatrix} \begin{bmatrix} pi_{dr1} \\ pi_{qr1} \\ pi_{0r1} \end{bmatrix} + \begin{bmatrix} -L_m\omega_r \sin(2\theta_r) & L_m\omega_r \cos(2\theta_r) & \sqrt{2}L_m\omega_r \sin(\theta_r) \\ L_m\omega_r \cos(2\theta_r) & L_m\omega_r \sin(2\theta_r) & -\sqrt{2}L_m\omega_r \cos(\theta_r) \\ 0 & 0 & 0 \end{bmatrix} \begin{bmatrix} i_{dr1} \\ i_{qr1} \\ i_{0r1} \end{bmatrix} \tag{22}$$

$$\begin{bmatrix} v_{dr1} \\ v_{qr1} \\ v_{0r1} \end{bmatrix} = \begin{bmatrix} r_r & 0 & 0 \\ 0 & r_r & 0 \\ 0 & 0 & r_r \end{bmatrix} \begin{bmatrix} i_{dr1} \\ i_{qr1} \\ i_{0r1} \end{bmatrix} + \begin{bmatrix} L_{lr}+L_m cos^2(\theta_r) & 0.5L_m \sin(2\theta_r) & -\sqrt{2}L_m \cos(\theta_r) \\ 0.5L_m \sin(2\theta_r) & L_{lr}+L_m sin^2(\theta_r) & -\sqrt{2}L_m \sin(\theta_r) \\ 0 & 0 & L_{lr} \end{bmatrix} \begin{bmatrix} pi_{dr1} \\ pi_{qr1} \\ pi_{0r1} \end{bmatrix} + \begin{bmatrix} -0.5L_m\omega_r \sin(2\theta_r) & L_{lr}\omega_r + L_m\omega_r cos^2(\theta_r) & 0 \\ -L_{lr}\omega_r - L_m\omega_r sin^2(\theta_r) & 0.5L_m\omega_r \sin(2\theta_r) & 0 \\ 0 & 0 & 0 \end{bmatrix} \begin{bmatrix} i_{dr1} \\ i_{qr1} \\ i_{0r1} \end{bmatrix} + \begin{bmatrix} L_m & 0 & -\sqrt{2}L_m \\ 0 & 0 & 0 \\ 0 & 0 & 0 \end{bmatrix} \begin{bmatrix} pi_{ds1} \\ pi_{qs1} \\ pi_{0s1} \end{bmatrix} + \begin{bmatrix} 0 & 0 & 0 \\ -L_m\omega_r & 0 & \sqrt{2}L_m\omega_r \\ 0 & 0 & 0 \end{bmatrix} \begin{bmatrix} i_{ds1} \\ i_{qs1} \\ i_{0s1} \end{bmatrix} \tag{23}$$

From (22) and (23), electromagnetic torque ($T_{e\text{-}I}$) is obtained for the first part as shown in (24).

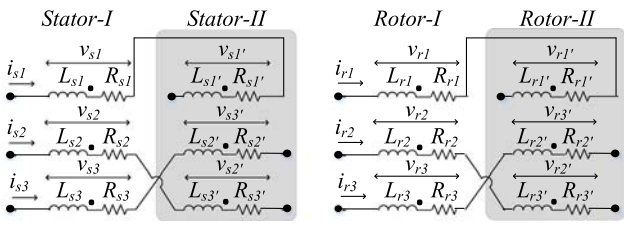

Figure 11. Case-IV: Stator and rotor windings.

$$\begin{aligned} T_{e-I} = (P/2)\big[&-L_m \sin(2\theta_r) i_{ds1} i_{dr1} + L_m \cos(2\theta_r) i_{ds1} i_{qr1} \\ &+\sqrt{2}L_m \sin(\theta_r) i_{ds1} i_{0r1} \\ &+ L_m \cos(2\theta_r) i_{qs1} i_{dr1} + L_m \sin(2\theta_r) i_{qs1} i_{qr1} \\ &- \sqrt{2}L_m \cos(\theta_r) i_{qs1} i_{0r1} - 0.5L_m \sin(2\theta_r) i_{dr1}^2 \\ &+ 0.5L_m \sin(2\theta_r) i_{qr1}^2 + L_m \cos(2\theta_r) i_{dr1} i_{qr1} - L_m i_{ds1} i_{qr1} \\ &+ \sqrt{2}L_m i_{0s1} i_{qr1}\big] \end{aligned} \tag{24}$$

For the stator-II and rotor-II, voltage equations are similar to (22), and (23) but having voltage and current with subscript of '2' as in case-III. Therefore ($T_{e\text{-}II}$) can be written as (25).

$$\begin{aligned} T_{e-II} = (P/2)\big[&-L_m \sin(2\theta_r) i_{ds2} i_{dr2} + L_m \cos(2\theta_r) i_{ds2} i_{qr2} \\ &+ \sqrt{2}L_m \sin(\theta_r) i_{ds2} i_{0r2} \\ &+ L_m \cos(2\theta_r) i_{qs2} i_{dr2} + L_m \sin(2\theta_r) i_{qs2} i_{qr2} \\ &- \sqrt{2}L_m \cos(\theta_r) i_{qs2} i_{0r2} - 0.5L_m \sin(2\theta_r) i_{dr2}^2 \\ &+ 0.5L_m \sin(2\theta_r) i_{qr2}^2 + L_m \cos(2\theta_r) i_{dr2} i_{qr2} - L_m i_{ds2} i_{qr2} \\ &+ \sqrt{2}L_m i_{0s2} i_{qr2}\big] \end{aligned} \tag{25}$$

Now, total electromagnetic torque is calculated by adding (24) and (25), with the help of (19).

$$\begin{aligned} T_e = (P/2)\big[&2L_m \sin(2\theta_r)\left(i_{qs} i_{qr} - i_{ds} i_{dr}\right) \\ &+2\sqrt{2}L_m \sin(\theta_r) i_{ds} i_{0r} + L_m \sin(2\theta_r)\left(i_{qr}^2 - i_{dr}^2\right)\big] \end{aligned} \tag{26}$$

In balanced currents, i_0 component is zero. Therefore, torque (26) is one third of case-III (20) as shown in figure 12. It is observed from figure 4(d) that the magnitude of pulsating field is also one third from the case-III as shown in figure 4(c).

4. Experimantal results

Winding configurations developed for the IBC are verified on the experimental setup with four pole IM of 2 hp having 415 V, 50 Hz and 3 A rating. A schematic diagram is shown in figure 13(a) with STP-IM and the experimental rig is shown in figure 13(b). The current flowing through windings for different cases are measured. Speed response is

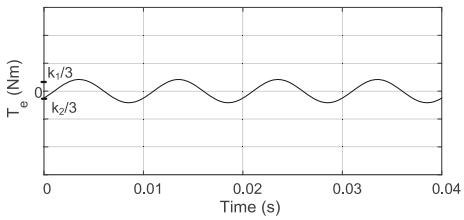

Figure 12. Case-IV: Electromagnetic torque.

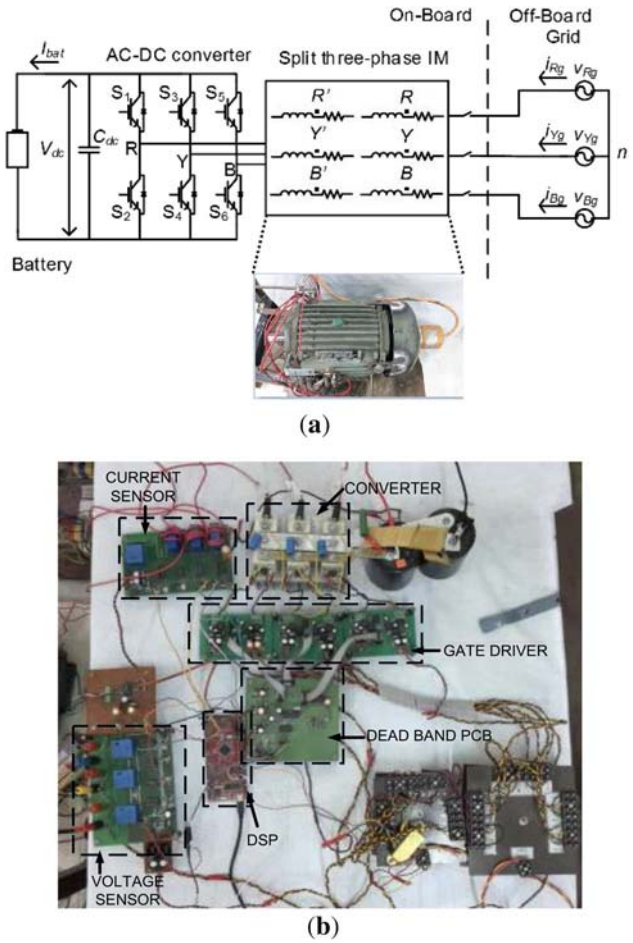

Figure 13. (a) Schematic diagram and (b) Experimental rig.

observed by using EN 801-1500 shaft encoder and captured with onboard DAC of Texas Instruments digital signal processor (TMS320F28377S). The voltage equations (in abc-form) written for the respective cases, provides the equivalent inductance values which can be used for filtering purpose.

In case-I, inductance provided by windings is high and balanced as seen from (27). Therefore, current has a balanced nature with low total harmonic distortion (THD) however the rotor of machine rotates. Hence it is not used for filtering operation. Current and speed waveform for case-I is shown in figure 14(a). As observed from voltage equation (29) only leakage inductance is responsible for filtering operation in case-II winding connections. These inductances are balanced in all phases but have low values, therefore balanced current with high THD is observed. The case-II connection do not generate electromagnetic torque in rotor, therefore, speed of rotor is zero as shown in figure 14(b).

Winding impedances of case-III are unbalanced as noticed in voltage equation (31). Y-phase and B-phase have same but lower value of inductance than R-phase. Winding current and speed of rotor for case-III is shown in figure 14(c). It observed that rotor is standstill, with R-phase having lower current with lower THD. This unbalance in winding current is generated by the presence of PMF in machine. For the case-IV, magnitude of PMF developed along R-phase is reduced by connecting the R-phase winding with *opposite sense of orientation*. As the magnitude of PMF is reduced, the unbalance in winding current is also reduced and rotor is also standstill as shown in figure 14(d). Table 1 shows the X/R ratio of the winding.

These values are obtained by performing the block rotor test on the machine. The value of winding current with its THD in respective phases observed during the experimentation are also shown in table 1. Case-I have balanced current with low THD, but rotor is not stationary. Case-II also shows the balanced current with electromagnetic torque equal to zero but have high THD. Case-III have unbalanced currents due to PMF effect. In the case-IV, PMF effect is reduced therefore the unbalance in winding current is also reduced. Among all cases in which rotor is stationary, case-III has high X/R ratio. However, THD in the grid current is high because of the unbalanced nature of the filter impedances [29]. The grid current THD and power factor correction due to this unbalance can be reduced by using various algorithms, as explained in [28, 29].

5. Conclusion

In this paper, STP-IM as a grid interfacing inductor between the grid and converter is discussed. Various winding configurations are proposed that could be used for IBC. A mathematical investigation is presented which indicates the nature of torque produced in the winding connections. Derived torque equations provide the mathematical proof for the stand stillness of the rotor. In those connections where PMF is present, pulsating torque is observed which is also incapable to rotate the rotor. Hence mechanical braking is not required. As the magnitude of PMF is reduced, the pulsation in electromagnetic torque is also reduced. The presented experimental results for winding current and speed of the machine for all developed cases verifies the numerical investigation. The presence of

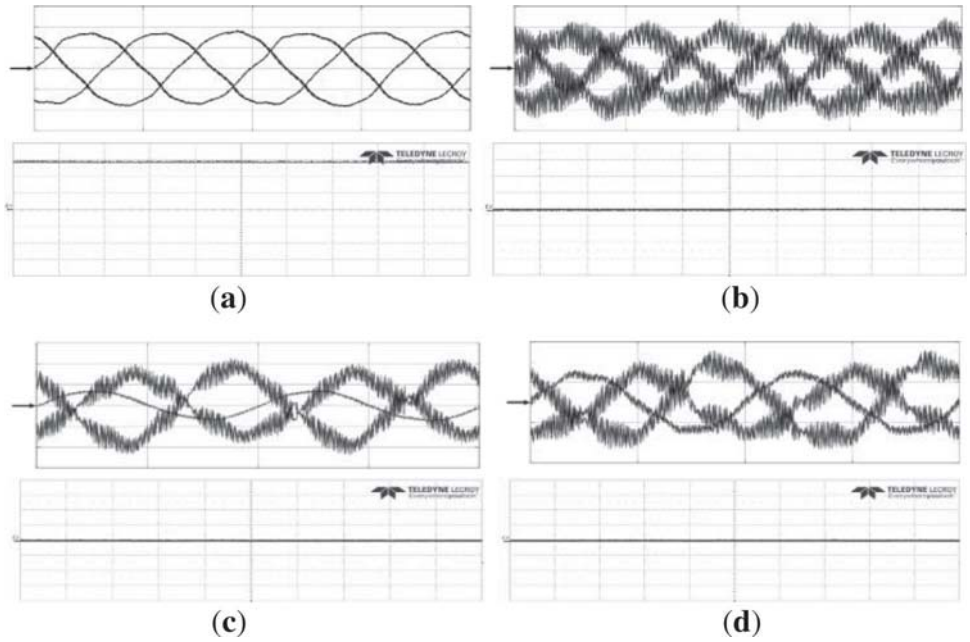

Figure 14. Current flowing through windings and motor speed: (a) Case-I, (b) Case-II, (c) Case-III, (d) Case-IV [Scale – x: axis 0.01ms/div, Stator current – y: axis 0.8A/div, Speed – y: axis 500rpm/div].

Table 1. X/R ratio for all cases.

	X/R ratio			Winding current (A)			THD (%)		
Cases	R	Y	B	R	Y	B	R	Y	B
I				1.00	0.96	0.97	3.28	4.35	3.69
II	0.077	0.072	0.073	0.94	1.02	0.95	12.3	13.19	14.96
III	1.126	0.704	0.753	0.38	0.92	1.02	4.19	14.06	12.75
IV	0.061	0.535	0.546	0.78	0.82	1.02	8.35	15.94	15.52

PMF changes the equivalent impedance provided by machine windings during charging mode. The most preferable connection is case-III, as it provides the better X/R ratio which could be used judicially in IBC.

Acknowledgements

This work was supported by the Visvesvaraya PhD scheme, Ministry of Electronics and Information Technology (MeitY), Government of India, under Grant PhD MLA/4{14}/2015-16.

List of symbols

$[v_s]$, $[v_r]$	Stator and rotor phase voltage
$[i_s]$, $[i_r]$	Stator and rotor phase current
$[R_s]$, $[R_r]$	Stator and rotor resistance
$[L_{ss}]$, $[L_{rr}]$	Stator and rotor inductance
$[L_{sr}]$, $[L_{rs}]$	Mutual inductance between stator and rotor and vice versa
v_{kl}	Voltage across winding (k = s, r for stator (s), and rotor (r) and l=1, 2, 3 represents the winding number)
i_{kl}	Current flowing through winding
R_{kl}	Winding resistance
L_{kl}	Winding self-inductance
M_{klkl}	Winding mutual-inductance
θ_r	Angular position between stator and rotor axes
ω_r	Rotor angular speed

Appendix A

By using below terms in (1), and (2), voltage equation for the stator and rotor can be written as (27) and (28), respectively. Then finally voltage equations (8), (9) in dq-frame are obtained for the case-I.

$$[v_s] = \begin{bmatrix} v_{s1} + v_{s1'} \\ v_{s2} + v_{s2'} \\ v_{s3} + v_{s3'} \end{bmatrix}, \quad [v_r] = \begin{bmatrix} v_{r1} + v_{r1'} \\ v_{r2} + v_{r2'} \\ v_{r3} + v_{r3'} \end{bmatrix},$$

$$[i_s] = \begin{bmatrix} i_{s1} \\ i_{s2} \\ i_{s3} \end{bmatrix},$$

$$[R_s] = \begin{bmatrix} R_{s1} + R_{s1'} & 0 & 0 \\ 0 & R_{s2} + R_{s2'} & 0 \\ 0 & 0 & R_{s3} + R_{s3'} \end{bmatrix},$$

$$[i_r] = \begin{bmatrix} i_{r1} \\ i_{r2} \\ i_{r3} \end{bmatrix},$$

$$[R_r] = \begin{bmatrix} R_{r1} + R_{r1'} & 0 & 0 \\ 0 & R_{r2} + R_{r2'} & 0 \\ 0 & 0 & R_{r3} + R_{r3'} \end{bmatrix},$$

Appendix B

Terms $[v_s]$, $[v_r]$, $[i_s]$, $[i_r]$, $[R_s]$ and $[R_r]$ are same as case-I. But inductance matrices are modified for case-II as shown in bottom of next page.

Therefore, voltage equation for the case-II can be written as (29) and (30) for the stator and rotor respectively.

$$[v_s] = \begin{bmatrix} 2r_s & 0 & 0 \\ 0 & 2r_s & 0 \\ 0 & 0 & 2r_s \end{bmatrix} \begin{bmatrix} i_{s1} \\ i_{s2} \\ i_{s3} \end{bmatrix} + p\left(\begin{bmatrix} 2L_{ls} & 0 & 0 \\ 0 & 2L_{ls} & 0 \\ 0 & 0 & 2L_{ls} \end{bmatrix} \begin{bmatrix} i_{s1} \\ i_{s2} \\ i_{s3} \end{bmatrix} \right) + p\left(\begin{bmatrix} 0 & 0 & 0 \\ 0 & 0 & 0 \\ 0 & 0 & 0 \end{bmatrix} \begin{bmatrix} i_{r1} \\ i_{r2} \\ i_{r3} \end{bmatrix} \right) \tag{29}$$

$$[L_{ss}] = \begin{bmatrix} L_{s1} + M_{s1s1'} + L_{s1'} + M_{s1's1} & M_{s1s2} + M_{s1s2'} + M_{s1's2} + M_{s1's2'} & M_{s1s3} + M_{s1s3'} + M_{s1's3} + M_{s1's3'} \\ M_{s2s1} + M_{s2s1'} + M_{s2's1} + M_{s2's1'} & L_{s2} + M_{s2s2'} + L_{s2'} + M_{s2's2} & M_{s2s3} + M_{s2s3'} + M_{s2's3} + M_{s2's3'} \\ M_{s3s1} + M_{s3s1'} + M_{s3's1} + M_{s3's1'} & M_{s3s2} + M_{s3s2'} + M_{s3's2} + M_{s3's2'} & L_{s3} + M_{s3s3'} + L_{s3'} + M_{s3's3} \end{bmatrix}$$

$$[L_{sr}] = \begin{bmatrix} M_{s1r1} + M_{s1r1'} + M_{s1'r1} + M_{s1'r1'} & M_{s1r2} + M_{s1r2'} + M_{s1'r2} + M_{s1'r2'} & M_{s1r3} + M_{s1r3'} + M_{s1'r3} + M_{s1'r3'} \\ M_{s2r1} + M_{s2r1'} + M_{s2'r1} + M_{s2'r1'} & M_{s2r2} + M_{s2r2'} + M_{s2'r2} + M_{s2'r2'} & M_{s2r3} + M_{s2r3'} + M_{s2'r3} + M_{s2'r3'} \\ M_{s3r1} + M_{s3r1'} + M_{s3'r1} + M_{s3'r1'} & M_{s3r2} + M_{s3r2'} + M_{s3'r2} + M_{s3'r2'} & M_{s3r3} + M_{s3r3'} + M_{s3'r3} + M_{s3'r3'} \end{bmatrix}$$

$$[L_{rr}] = \begin{bmatrix} L_{r1} + M_{r1r1'} + L_{r1'} + M_{r1'r1} & M_{r1r2} + M_{r1r2'} + M_{r1'r2} + M_{r1'r2'} & M_{r1r3} + M_{r1r3'} + M_{r1'r3} + M_{r1'r3'} \\ M_{r2r1} + M_{r2r1'} + M_{r2'r1} + M_{r2'r1'} & L_{r2} + M_{r2r2'} + L_{r2'} + M_{r2'r2} & M_{r2r3} + M_{r2r3'} + M_{r2'r3} + M_{r2'r3'} \\ M_{r3r1} + M_{r3r1'} + M_{r3'r1} + M_{r3'r1'} & M_{r3r2} + M_{r3r2'} + M_{r3'r2} + M_{r3'r2'} & L_{r3} + M_{r3r3'} + L_{r3'} + M_{r3'r3} \end{bmatrix}$$

$$[L_{rs}] = \begin{bmatrix} M_{r1s1} + M_{r1s1'} + M_{r1's1} + M_{r1's1'} & M_{r1s2} + M_{r1s2'} + M_{r1's2} + M_{r1's2'} & M_{r1s3} + M_{r1s3'} + M_{r1's3} + M_{r1's3'} \\ M_{r2s1} + M_{r2s1'} + M_{r2's1} + M_{r2's1'} & M_{r2s2} + M_{r2s2'} + M_{r2's2} + M_{r2's2'} & M_{r2s3} + M_{r2s3'} + M_{r2's3} + M_{r2's3'} \\ M_{r3s1} + M_{r3s1'} + M_{r3's1} + M_{r3's1'} & M_{r3s2} + M_{r3s2'} + M_{r3's2} + M_{r3's2'} & M_{r3s3} + M_{r3s3'} + M_{r3's3} + M_{r3's3'} \end{bmatrix}$$

$$[v_s] = \begin{bmatrix} 2r_s & 0 & 0 \\ 0 & 2r_s & 0 \\ 0 & 0 & 2r_s \end{bmatrix} \begin{bmatrix} i_{s1} \\ i_{s2} \\ i_{s3} \end{bmatrix} + p\left(\begin{bmatrix} 2L_{ls} + 4L_m & -2L_m & -2L_m \\ -2L_m & 2L_{ls} + 4L_m & -2L_m \\ -2L_m & -2L_m & 2L_{ls} + 4L_m \end{bmatrix} \begin{bmatrix} i_{s1} \\ i_{s2} \\ i_{s3} \end{bmatrix} \right) + p\left(\begin{bmatrix} 4L_m \cos(\theta_r) & 4L_m \cos\left(\theta_r + 2\pi/3\right) & 4L_m \cos\left(\theta_r + 4\pi/3\right) \\ 4L_m \cos\left(\theta_r + 4\pi/3\right) & 4L_m \cos(\theta_r) & 4L_m \cos\left(\theta_r + 2\pi/3\right) \\ 4L_m \cos\left(\theta_r + 2\pi/3\right) & 4L_m \cos\left(\theta_r + 4\pi/3\right) & 4L_m \cos(\theta_r) \end{bmatrix} \begin{bmatrix} i_{r1} \\ i_{r2} \\ i_{r3} \end{bmatrix} \right) \tag{27}$$

$$[v_r] = \begin{bmatrix} 2r_r & 0 & 0 \\ 0 & 2r_r & 0 \\ 0 & 0 & 2r_r \end{bmatrix} \begin{bmatrix} i_{r1} \\ i_{r2} \\ i_{r3} \end{bmatrix} + p\left(\begin{bmatrix} 2L_{lr} + 4L_m & -2L_m & -2L_m \\ -2L_m & 2L_{lr} + 4L_m & -2L_m \\ -2L_m & -2L_m & 2L_{lr} + 4L_m \end{bmatrix} \begin{bmatrix} i_{r1} \\ i_{r2} \\ i_{r3} \end{bmatrix} \right) + p\left(\begin{bmatrix} 4L_m \cos(-\theta_r) & 4L_m \cos\left(-\theta_r + 2\pi/3\right) & 4L_m \cos\left(-\theta_r + 4\pi/3\right) \\ 4L_m \cos\left(-\theta_r + 4\pi/3\right) & 4L_m \cos(-\theta_r) & 4L_m \cos\left(-\theta_r + 2\pi/3\right) \\ 4L_m \cos\left(-\theta_r + 2\pi/3\right) & 4L_m \cos\left(-\theta_r + 4\pi/3\right) & 4L_m \cos(-\theta_r) \end{bmatrix} \begin{bmatrix} i_{s1} \\ i_{s2} \\ i_{s3} \end{bmatrix} \right) \tag{28}$$

$$[v_r] = \begin{bmatrix} 2r_r & 0 & 0 \\ 0 & 2r_r & 0 \\ 0 & 0 & 2r_r \end{bmatrix} \begin{bmatrix} i_{r1} \\ i_{r2} \\ i_{r3} \end{bmatrix} + p\left(\begin{bmatrix} 2L_{lr} & 0 & 0 \\ 0 & 2L_{lr} & 0 \\ 0 & 0 & 2L_{lr} \end{bmatrix} \begin{bmatrix} i_{r1} \\ i_{r2} \\ i_{r3} \end{bmatrix} \right) + p\left(\begin{bmatrix} 0 & 0 & 0 \\ 0 & 0 & 0 \\ 0 & 0 & 0 \end{bmatrix} \begin{bmatrix} i_{s1} \\ i_{s2} \\ i_{s3} \end{bmatrix} \right) \quad (30)$$

Transform (29), (30) to stationary dq-frame with fictitious rotor axes gives (12), (13).

Appendix C

In case-III, stator-I and rotor-I windings, terms for voltage equations (1), and (2) are mentioned below:

$$[v_s] = \begin{bmatrix} v_{s1} \\ v_{s2} \\ v_{s3} \end{bmatrix}, \quad [v_r] = \begin{bmatrix} v_{r1} \\ v_{r2} \\ v_{r3} \end{bmatrix}, \quad [i_s] = \begin{bmatrix} i_{s1} \\ i_{s2} \\ i_{s3} \end{bmatrix}, \quad [i_r] = \begin{bmatrix} i_{r1} \\ i_{r2} \\ i_{r3} \end{bmatrix},$$

$$[R_s] = \begin{bmatrix} R_{s1} & 0 & 0 \\ 0 & R_{s2} & 0 \\ 0 & 0 & R_{s3} \end{bmatrix}, \quad [R_r] = \begin{bmatrix} R_{r1} & 0 & 0 \\ 0 & R_{r2} & 0 \\ 0 & 0 & R_{r3} \end{bmatrix},$$

$$[L_{ss}] = \begin{bmatrix} L_{s1} + M_{s1s1'} & M_{s1s2} + M_{s1s3'} & M_{s1s3} + M_{s1s2'} \\ M_{s2s1} + M_{s2s1'} & L_{s2} + M_{s2s3'} & M_{s2s3} + M_{s2s2'} \\ M_{s3s1} + M_{s3s1'} & M_{s3s2} + M_{s3s3'} & L_{s3} + M_{s3s2'} \end{bmatrix}$$

$$[L_{sr}] = \begin{bmatrix} M_{s1r1} + M_{s1r1'} & M_{s1r2} + M_{s1r3'} & M_{s1r3} + M_{s1r2'} \\ M_{s2r1} + M_{s2r1'} & M_{s2r2} + M_{s2r3'} & M_{s2r3} + M_{s2r2'} \\ M_{s3r1} + M_{s3r1'} & M_{s3r2} + M_{s3r3'} & M_{s3r3} + M_{s3r2'} \end{bmatrix}$$

$$[L_{rr}] = \begin{bmatrix} L_{r1} + M_{r1r1'} & M_{r1r2} + M_{r1r3'} & M_{r1r3} + M_{r1r2'} \\ M_{r2r1} + M_{r2r1'} & L_{r2} + M_{r2r3'} & M_{r2r3} + M_{r2r2'} \\ M_{r3r1} + M_{r3r1'} & M_{r3r2} + M_{r3r3'} & L_{r3} + M_{r3r2'} \end{bmatrix}$$

$$[L_{rs}] = \begin{bmatrix} M_{r1s1} + M_{r1s1'} & M_{r1s2} + M_{r1s3'} & M_{r1s3} + M_{r1s2'} \\ M_{r2s1} + M_{r2s1'} & M_{r2s2} + M_{r2s3'} & M_{r2s3} + M_{r2s2'} \\ M_{r3s1} + M_{r3s1'} & M_{r3s2} + M_{r3s3'} & M_{r3s3} + M_{r3s2'} \end{bmatrix}$$

Hence, equation for stator voltage (31) and for rotor voltage (32) is obtained. By transform to stationary dq-frame (15) and (16) will be obtained.

For stator-II and rotor-II, voltage equations are developed. Here supply phase-sequence is reversed, therefore terms are changed to following:

$$[v_s] = \begin{bmatrix} v_{s1'} \\ v_{s3'} \\ v_{s2'} \end{bmatrix}, \quad [v_r] = \begin{bmatrix} v_{r1'} \\ v_{r3'} \\ v_{r2'} \end{bmatrix}, \quad [i_s] = \begin{bmatrix} i_{s1} \\ i_{s3} \\ i_{s2} \end{bmatrix}, \quad [i_r] = \begin{bmatrix} i_{r1} \\ i_{r3} \\ i_{r2} \end{bmatrix},$$

$$[R_s] = \begin{bmatrix} R_{s1'} & 0 & 0 \\ 0 & R_{s2'} & 0 \\ 0 & 0 & R_{s3'} \end{bmatrix}, \quad [R_r] = \begin{bmatrix} R_{r1'} & 0 & 0 \\ 0 & R_{r2'} & 0 \\ 0 & 0 & R_{r3'} \end{bmatrix},$$

$$[L_{ss}] = \begin{bmatrix} L_{s1'} + M_{s1's1} & M_{s1's2'} + M_{s1's3} & M_{s1's3'} + M_{s1's2} \\ M_{s2's1'} + M_{s2's1} & L_{s2'} + M_{s2's3} & M_{s2's3'} + M_{s2's2} \\ M_{s3's1'} + M_{s3's1} & M_{s3's2'} + M_{s3's3} & L_{s3'} + M_{s3's2} \end{bmatrix}$$

$$[L_{sr}] = \begin{bmatrix} M_{s1'r1'} + M_{s1'r1} & M_{s1'r2'} + M_{s1'r3} & M_{s1'r3'} + M_{s1'r2} \\ M_{s2'r1'} + M_{s2'r1} & M_{s2'r2'} + M_{s2'r3} & M_{s2'r3'} + M_{s2'r2} \\ M_{s3'r1'} + M_{s3'r1} & M_{s3'r2'} + M_{s3'r3} & M_{s3'r3'} + M_{s3'r2} \end{bmatrix}$$

$$[L_{rr}] = \begin{bmatrix} L_{r1'} + M_{r1'r1} & M_{r1'r2'} + M_{r1'r3} & M_{r1'r3'} + M_{r1'r2} \\ M_{r2'r1'} + M_{r2'r1} & L_{r2'} + M_{r2'r3} & M_{r2'r3'} + M_{r2'r2} \\ M_{r3'r1'} + M_{r3'r1} & M_{r3'r2'} + M_{r3'r3} & L_{r3'} + M_{r3'r2} \end{bmatrix}$$

$$[L_{rs}] = \begin{bmatrix} M_{r1's1'} + M_{r1's1} & M_{r1's2'} + M_{r1's3} & M_{r1's3'} + M_{r1's2} \\ M_{r2's1'} + M_{r2's1} & M_{r2's2'} + M_{r2's3} & M_{r2's3'} + M_{r2's2} \\ M_{r3's1'} + M_{r3's1} & M_{r3's2'} + M_{r3's3} & M_{r3's3'} + M_{r3's2} \end{bmatrix}$$

$$[L_{ss}] = \begin{bmatrix} L_{s1} - M_{s1s1'} + L_{s1'} - M_{s1's1} & M_{s1s2} - M_{s1s2'} - M_{s1's2} + M_{s1's2'} & M_{s1s3} - M_{s1s3'} - M_{s1's3} + M_{s1's3'} \\ M_{s2s1} - M_{s2s1'} - M_{s2's1} + M_{s2's1'} & L_{s2} - M_{s2s2'} + L_{s2'} - M_{s2's2} & M_{s2s3} - M_{s2s3'} - M_{s2's3} + M_{s2's3'} \\ M_{s3s1} - M_{s3s1'} - M_{s3's1} + M_{s3's1'} & M_{s3s2} - M_{s3s2'} - M_{s3's2} + M_{s3's2'} & L_{s3} - M_{s3s3'} + L_{s3'} - M_{s3's3} \end{bmatrix}$$

$$[L_{sr}] = \begin{bmatrix} M_{s1r1} - M_{s1r1'} - M_{s1'r1} + M_{s1'r1'} & M_{s1r2} - M_{s1r2'} - M_{s1'r2} + M_{s1'r2'} & M_{s1r3} - M_{s1r3'} - M_{s1'r3} + M_{s1'r3'} \\ M_{s2r1} - M_{s2r1'} - M_{s2'r1} + M_{s2'r1'} & M_{s2r2} - M_{s2r2'} - M_{s2'r2} + M_{s2'r2'} & M_{s2r3} - M_{s2r3'} - M_{s2'r3} + M_{s2'r3'} \\ M_{s3r1} - M_{s3r1'} - M_{s3'r1} + M_{s3'r1'} & M_{s3r2} - M_{s3r2'} - M_{s3'r2} + M_{s3'r2'} & M_{s3r3} - M_{s3r3'} - M_{s3'r3} + M_{s3'r3'} \end{bmatrix}$$

$$[L_{rr}] = \begin{bmatrix} L_{r1} - M_{r1r1'} + L_{r1'} - M_{r1'r1} & M_{r1r2} - M_{r1r2'} - M_{r1'r2} + M_{r1'r2'} & M_{r1r3} - M_{r1r3'} - M_{r1'r3} + M_{r1'r3'} \\ M_{r2r1} - M_{r2r1'} - M_{r2'r1} + M_{r2'r1'} & L_{r2} - M_{r2r2'} + L_{r2'} - M_{r2'r2} & M_{r2r3} - M_{r2r3'} - M_{r2'r3} + M_{r2'r3'} \\ M_{r3r1} - M_{r3r1'} - M_{r3'r1} + M_{r3'r1'} & M_{r3r2} - M_{r3r2'} - M_{r3'r2} + M_{r3'r2'} & L_{r3} - M_{r3r3'} + L_{r3'} - M_{r3'r3} \end{bmatrix}$$

$$[L_{rs}] = \begin{bmatrix} M_{r1s1} - M_{r1s1'} - M_{r1's1} + M_{r1's1'} & M_{r1s2} - M_{r1s2'} - M_{r1's2} + M_{r1's2'} & M_{r1s3} - M_{r1s3'} - M_{r1's3} + M_{r1's3'} \\ M_{r2s1} - M_{r2s1'} - M_{r2's1} + M_{r2's1'} & M_{r2s2} - M_{r2s2'} - M_{r2's2} + M_{r2's2'} & M_{r2s3} - M_{r2s3'} - M_{r2's3} + M_{r2's3'} \\ M_{r3s1} - M_{r3s1'} - M_{r3's1} + M_{r3's1'} & M_{r3s2} - M_{r3s2'} - M_{r3's2} + M_{r3's2'} & M_{r3s3} - M_{r3s3'} - M_{r3's3} + M_{r3's3'} \end{bmatrix}$$

Appendix D

From the following values for case-IV, voltage equation for stator-I and rotor-I is given by (22) and (23) respectively, in stationary dq-frame.

$$[v_s] = \begin{bmatrix} v_{s1} \\ v_{s2} \\ v_{s3} \end{bmatrix}, \quad [v_r] = \begin{bmatrix} v_{r1} \\ v_{r2} \\ v_{r3} \end{bmatrix}, \quad [i_s] = \begin{bmatrix} i_{s1} \\ i_{s2} \\ i_{s3} \end{bmatrix}, \quad [i_r] = \begin{bmatrix} i_{r1} \\ i_{r2} \\ i_{r3} \end{bmatrix},$$

$$[R_s] = \begin{bmatrix} R_{s1} & 0 & 0 \\ 0 & R_{s2} & 0 \\ 0 & 0 & R_{s3} \end{bmatrix}, \quad [R_r] = \begin{bmatrix} R_{r1} & 0 & 0 \\ 0 & R_{r2} & 0 \\ 0 & 0 & R_{r3} \end{bmatrix}$$

$$[L_{ss}] = \begin{bmatrix} L_{s1} - M_{s1s1'} & M_{s1s2} + M_{s1s3'} & M_{s1s3} + M_{s1s2'} \\ M_{s2s1} - M_{s2s1'} & L_{s2} + M_{s2s3'} & M_{s2s3} + M_{s2s2'} \\ M_{s3s1} - M_{s3s1'} & M_{s3s2} + M_{s3s3'} & L_{s3} + M_{s3s2'} \end{bmatrix}$$

$$[L_{sr}] = \begin{bmatrix} M_{s1r1} - M_{s1r1'} & M_{s1r2} + M_{s1r3'} & M_{s1r3} + M_{s1r2'} \\ M_{s2r1} - M_{s2r1'} & M_{s2r2} + M_{s2r3'} & M_{s2r3} + M_{s2r2'} \\ M_{s3r1} - M_{s3r1'} & M_{s3r2} + M_{s3r3'} & M_{s3r3} + M_{s3r2'} \end{bmatrix}$$

$$[L_{rr}] = \begin{bmatrix} L_{r1} - M_{r1r1'} & M_{r1r2} + M_{r1r3'} & M_{r1r3} + M_{r1r2'} \\ M_{r2r1} - M_{r2r1'} & L_{r2} + M_{r2r3'} & M_{r2r3} + M_{r2r2'} \\ M_{r3r1} - M_{r3r1'} & M_{r3r2} + M_{r3r3'} & L_{r3} + M_{r3r2'} \end{bmatrix}$$

$$[L_{rs}] = \begin{bmatrix} M_{r1s1} - M_{r1s1'} & M_{r1s2} + M_{r1s3'} & M_{r1s3} + M_{r1s2'} \\ M_{r2s1} - M_{r2s1'} & M_{r2s2} + M_{r2s3'} & M_{r2s3} + M_{r2s2'} \\ M_{r3s1} - M_{r3s1'} & M_{r3s2} + M_{r3s3'} & M_{r3s3} + M_{r3s2'} \end{bmatrix}$$

Similarly, equations are also developed for stator-II and rotor-II by using the following variables. Here, current flowing in the second R-phase winding is in opposite direction. Therefore, i_{s1} and i_{r1} currents are replaced by $-i_{s1}$ and $-i_{r1}$ respectively.

$$[v_s] = \begin{bmatrix} v_{s1'} \\ v_{s3'} \\ v_{s2'} \end{bmatrix}, \quad [v_r] = \begin{bmatrix} v_{r1'} \\ v_{r3'} \\ v_{r2'} \end{bmatrix}, \quad [i_s] = \begin{bmatrix} -i_{s1} \\ i_{s3} \\ i_{s2} \end{bmatrix}, \quad [i_r] = \begin{bmatrix} -i_{r1} \\ i_{r3} \\ i_{r2} \end{bmatrix},$$

$$[R_s] = \begin{bmatrix} R_{s1'} & 0 & 0 \\ 0 & R_{s2'} & 0 \\ 0 & 0 & R_{s3'} \end{bmatrix}, \quad [R_r] = \begin{bmatrix} R_{r1'} & 0 & 0 \\ 0 & R_{r2'} & 0 \\ 0 & 0 & R_{r3'} \end{bmatrix},$$

$$[L_{ss}] = \begin{bmatrix} L_{s1'} - M_{s1's1} & -M_{s1's2'} - M_{s1's3} & -M_{s1's3'} - M_{s1's2} \\ -M_{s2's1'} + M_{s2's1} & L_{s2'} + M_{s2's3} & M_{s2's3'} + M_{s2's2} \\ -M_{s3's1'} + M_{s3's1} & M_{s3's2'} + M_{s3's3} & L_{s3'} + M_{s3's2} \end{bmatrix}$$

$$[L_{sr}] = \begin{bmatrix} M_{s1'r1'} - M_{s1'r1} & -M_{s1'r2'} - M_{s1'r3} & -M_{s1'r3'} - M_{s1'r2} \\ -M_{s2'r1'} + M_{s2'r1} & M_{s2'r2'} + M_{s2'r3} & M_{s2'r3'} + M_{s2'r2} \\ -M_{s3'r1'} + M_{s3'r1} & M_{s3'r2'} + M_{s3'r3} & M_{s3'r3'} + M_{s3'r2} \end{bmatrix}$$

$$[L_{rr}] = \begin{bmatrix} L_{r1'} - M_{r1'r1} & -M_{r1'r2'} - M_{r1'r3} & -M_{r1'r3'} - M_{r1'r2} \\ -M_{r2'r1'} + M_{r2'r1} & L_{r2'} + M_{r2'r3} & M_{r2'r3'} + M_{r2'r2} \\ -M_{r3'r1'} + M_{r3'r1} & M_{r3'r2'} + M_{r3'r3} & L_{r3'} + M_{r3'r2} \end{bmatrix}$$

$$[L_{rs}] = \begin{bmatrix} M_{r1's1} - M_{r1's1'} & -M_{r1's2'} - M_{r1's3} & -M_{r1's3'} - M_{r1's2} \\ -M_{r2's1'} + M_{r2's1} & M_{r2's2'} + M_{r2's3} & M_{r2's3'} + M_{r2's2} \\ -M_{r3's1'} + M_{r3's1} & M_{r3's2'} + M_{r3's3} & M_{r3's3'} + M_{r3's2} \end{bmatrix}$$

$$\begin{bmatrix} v_{s1} \\ v_{s2} \\ v_{s3} \end{bmatrix} = \begin{bmatrix} r_s & 0 & 0 \\ 0 & r_s & 0 \\ 0 & 0 & r_s \end{bmatrix} \begin{bmatrix} i_{s1} \\ i_{s2} \\ i_{s3} \end{bmatrix} + p \left(\begin{bmatrix} L_{ls} + 2L_m & -L_m & -L_m \\ -L_m & L_{ls} + 0.5L_m & 0.5L_m \\ -L_m & 0.5L_m & L_{ls} + 0.5L_m \end{bmatrix} \begin{bmatrix} i_{s1} \\ i_{s2} \\ i_{s3} \end{bmatrix} \right) + p \left(L_m [Z_1] \begin{bmatrix} i_{r1} \\ i_{r2} \\ i_{r3} \end{bmatrix} \right) \quad (31)$$

$$Z_1 = \begin{bmatrix} 2\cos(\theta_r) & \cos\left(\theta_r + 2\pi/3\right) + \cos\left(\theta_r + 4\pi/3\right) & \cos\left(\theta_r + 4\pi/3\right) + \cos\left(\theta_r + 2\pi/3\right) \\ 2\cos\left(\theta_r + 4\pi/3\right) & \cos(\theta_r) + \cos\left(\theta_r + 2\pi/3\right) & \cos\left(\theta_r + 2\pi/3\right) + \cos(\theta_r) \\ 2\cos\left(\theta_r + 2\pi/3\right) & \cos\left(\theta_r + 4\pi/3\right) + \cos(\theta_r) & \cos(\theta_r) + \cos\left(\theta_r + 4\pi/3\right) \end{bmatrix}$$

$$\begin{bmatrix} v_{r1} \\ v_{r2} \\ v_{r3} \end{bmatrix} = \begin{bmatrix} r_r & 0 & 0 \\ 0 & r_r & 0 \\ 0 & 0 & r_r \end{bmatrix} \begin{bmatrix} i_{r1} \\ i_{r2} \\ i_{r3} \end{bmatrix} + p\left(\begin{bmatrix} L_{lr}+2L_m & -L_m & -L_m \\ -L_m & L_{lr}+0.5L_m & 0.5L_m \\ -L_m & 0.5L_m & L_{lr}+0.5L_m \end{bmatrix} \begin{bmatrix} i_{r1} \\ i_{r2} \\ i_{r3} \end{bmatrix} \right) + p\left(L_m[Z_2] \begin{bmatrix} i_{s1} \\ i_{s2} \\ i_{s3} \end{bmatrix} \right) \quad (32)$$

$$Z_2 = \begin{bmatrix} 2\cos(-\theta_r) & \cos\left(-\theta_r + {}^{2\pi}/_{3}\right) + \cos\left(-\theta_r + {}^{4\pi}/_{3}\right) & \cos\left(-\theta_r + {}^{4\pi}/_{3}\right) + \cos\left(-\theta_r + {}^{2\pi}/_{3}\right) \\ 2\cos\left(-\theta_r + {}^{4\pi}/_{3}\right) & \cos(-\theta_r) + \cos\left(-\theta_r + {}^{2\pi}/_{3}\right) & \cos\left(-\theta_r + {}^{2\pi}/_{3}\right) + \cos(-\theta_r) \\ 2\cos\left(-\theta_r + {}^{2\pi}/_{3}\right) & \cos\left(-\theta_r + {}^{4\pi}/_{3}\right) + \cos(-\theta_r) & \cos(-\theta_r) + \cos\left(-\theta_r + {}^{4\pi}/_{3}\right) \end{bmatrix}$$

References

[1] Yilmaz M and Krein P T 2013 Review of battery charger topologies, charging power levels, and infrastructure for plug-in electric and hybrid vehicles. *IEEE Trans. Power Electron.* 28(5): 2151–2169

[2] Yong Chen, Jun Zhou, Wen-Ping Dai and Eric Hu 2014 Application of improved bridgeless power factor correction based on one-cycle control in electric vehicle charging system. *Electric Power Compon. Syst.* (42)2: 112–123

[3] Lacressonniere F and Cassoret B 2005 Converter used as a battery charger and a motor speed controller in an industrial truck. In: *European Conference on Power Electronics and Applications.* Dresden 7

[4] Haghbin S, Lundmark S, Alakula M and Carlson O 2011 An isolated high-power integrated charger in electrified-vehicle applications. *IEEE Trans. Veh. Technol*. 60(9): 4115–4126

[5] Abdel Khalik A S, Massoud A and Ahmed S 2018 Interior permanent magnet motor-based isolated on-board integrated battery charger for electric vehicles. *IET Electric Power Appl.* 12(1): 124–134

[6] Shi C and Khaligh A 2018 A two-stage three-phase integrated charger for electric vehicles with dual cascaded control strategy. *IEEE J. Emerg. Sel. Top. Power Electron* 6(2): 898–909

[7] Pellegrino G, Armando E and Guglielmi P 2010 An integral battery charger with power factor correction for electric scooter. *IEEE Trans. Power Electron* 25(3): 751–759

[8] Liu T H, Chen Y, Yi P H and Chen J L 2015 Integrated battery charger with power factor correction for electric-propulsion systems. *IET Electric Power Appl*. 9(3): 229–238

[9] Shi C, Tang Y and Khaligh A 2018 A three-phase integrated onboard charger for plug-in electric vehicles. *IEEE Trans. Power Electron* 33(6): 4716–4725

[10] Sul Seung-Ki and Lee Sang-Joon 1995 An integral battery charger for four-wheel drive electric vehicle. *IEEE Trans. Ind. Appl.* 31(5): 1096–1099

[11] Subotic I, Bodo N and Levi E 2016 Single-phase on-board integrated battery chargers for EVs based on multiphase machines *IEEE Trans. Power Electron* 31(9): 6511–6523

[12] Khaligh A. and D'Antonio M 2019 Global trends in high-power on-board chargers for electric vehicles. *IEEE Trans. Veh. Technol.* 68(4): 3306–3324

[13] Continental CES 2018: Continental automates charging of electric vehicles and makes them a mobile power bank. https://www.continentalcorporation.com/en/press/press-releases/2017-12-13-ces-charging-116068

[14] Thimmesch D 1985 An SCR inverter with an integral battery charger for electric vehicles. *IEEE Trans. Ind. Appl.* 21(4): 1023–1029

[15] De Sousa L and Bouchez B 2010 Combined electric device for powering and charging WO2010057892

[16] De Sousa L and Bouchez B 2010 Method and electric combined device for powering and charging with compensation means WO2010057893

[17] De Sousa L, Bouchez B and Da Costa J L 2013 Method of exchanging electrical energy between an electrical network conveying a dc or ac electrical quantity and an electrical energy storage unit for hybrid or electric vehicle WO2013093287

[18] Bouchez B and De Sousa L 2014 Charge transfer device and associated management method US20140042807 A1

[19] Ali S Q, Mascarella D, Joos G and Tan L 2018 Torque cancelation of integrated battery charger based on six-phase permanent magnet synchronous motor drives for electric vehicles. *IEEE Trans. Transp. Electr.* 4(2): 344–354

[20] Zhihong Ye, Boroyevich D, Jae-Young Choi and Lee F C 2002 Control of circulating current in two parallel three-phase boost rectifiers. *IEEE Trans. Power Electron* 17(5): 609–615

[21] Renault Press Kit 2013. Renault ZOE: The electric supermini for every-day use. www.media.renault.com.

[22] Loudot S, Briane B, Ploix O and Villeneuve A 2012 Fast charging device for an electric vehicle U.S. Patent US 2012/0 286 740 A1

[23] Briane B and Loudot S. 2011 Rapid reversible charging device for an electric vehicle U.S. Patent US 2011/0 254 494 A1

[24] Bazzi A M, Liu Y and Fay D S 2018 electric machines and energy storage: over a century of technologies in electric and hybrid electric vehicles. *IEEE Electr. Mag.* 6(3): 49–53

[25] Lacroix S, Laboure E and Hilairet M 2010 An integrated fast battery charger for Electric Vehicle. In: *IEEE Vehicle Power and Propulsion Conference*, pp. 1–6

[26] Mengatto A and Heerdt J A 2017 Analysis and operation of an integrated battery charger using the EV traction motor as filter In: *Brazilian Power Electronics Conf. (COBEP)* 1-6

[27] Li C, Huang W, Cao R, Bu F and Fan C 2016 An integrated topology of charger and drive for electric buses. *IEEE Trans. Veh. Technol.* 65(6): 4471–4479

[28] Subotic I, Bodo N and Levi E 2017 Integration of six-phase EV drivetrains into battery charging process with direct grid connection. *IEEE Trans. Energy Convers.* 32(3): 1012–1022

[29] Suh Yongsug and Lipo T A 2006 Control scheme in hybrid synchronous stationary frame for PWM AC/DC converter under generalized unbalanced operating conditions. *IEEE Trans. Ind. Appl.* 42(3): 825–835